Higgs p_T Spectrum and Total Cross Section with Fiducial Cuts at Third Resummed and Fixed Order in QCD

Georgios Billis,[1] Bahman Dehnadi,[1] Markus A. Ebert,[2] Johannes K. L. Michel,[3] and Frank J. Tackmann[1]
[1]Deutsches Elektronen-Synchrotron (DESY), D-22607 Hamburg, Germany
[2]Max-Planck-Institut für Physik, Föhringer Ring 6, 80805 München, Germany
[3]Center for Theoretical Physics, Massachusetts Institute of Technology, Cambridge, Massachusetts 02139, USA

(Received 16 February 2021; revised 31 March 2021; accepted 7 July 2021; published 10 August 2021)

We present predictions for the gluon-fusion Higgs p_T spectrum at third resummed and fixed order (N^{3}LL$'$ + N^{3}LO) including fiducial cuts as required by experimental measurements at the Large Hadron Collider. Integrating the spectrum, we predict for the first time the total fiducial cross section to third order (N^{3}LO) and improved by resummation. The N^{3}LO correction is enhanced by cut-induced logarithmic effects and is not reproduced by the inclusive N^{3}LO correction times a lower-order acceptance. These are the highest-order predictions of their kind achieved so far at a hadron collider.

DOI: 10.1103/PhysRevLett.127.072001

Introduction.—Fiducial and differential cross-section measurements of the discovered Higgs boson [1,2] provide the most model-independent way to study Higgs production at the Large Hadron Collider. They are thus central to its physics program [3–15] and will remain so in the future [16].

Theoretical predictions for the dominant gluon-fusion ($gg \to H$) Higgs production mode suffer from large perturbative corrections. This has led to the calculation of the total inclusive production cross section to third order (N^{3}LO) [17–25], which is made possible by treating the decay of the Higgs boson fully inclusively. Unfortunately, this also makes it a primarily theoretical quantity, one that cannot be measured in experiment. The experimental measurements necessarily involve kinematic selection and acceptance cuts on the Higgs decay products, which reduce the cross section by an $\mathcal{O}(1)$ amount. Therefore, any comparison of theory and experiment always involves a prediction of the *fiducial* cross section, i.e., the cross section within the experimental acceptance. Currently, the fiducial cross section for $gg \to H$ is only know to second order (NNLO). A key challenge is to calculate it at N^{3}LO, which we do here for the first time. To be specific, we consider $H \to \gamma\gamma$ with the fiducial cuts used by ATLAS [8,26],

$$p_T^{\gamma 1} \geq 0.35 m_H, \qquad p_T^{\gamma 2} \geq 0.25 m_H,$$
$$|\eta^\gamma| \leq 1.37 \quad \text{or} \quad 1.52 \leq |\eta^\gamma| \leq 2.37. \tag{1}$$

Arguably, the most important differential cross section of the Higgs boson is its transverse-momentum (q_T) distribution, serving as a benchmark spectrum in many experimental analyses. At finite q_T, it is known to NNLO$_1$ [27–36], i.e., from calculating $H + 1$ parton to NNLO, including fiducial cuts, which is an important ingredient for our results. For $q_T \ll m_H$, the q_T spectrum contains large Sudakov logarithms of q_T/m_H, which must be resummed to all orders in perturbation theory to obtain precise and reliable predictions. So far, this resummation has been achieved to NNLL$'$ and N^{3}LL [37–44], which include second and third order evolution and which capture in particular all $\mathcal{O}(\alpha_s^2)$ contributions that are singular for $q_T \to 0$. This is also the basis of the q_T subtraction method for NNLO calculations [45].

In this Letter, we obtain for the first time the resummed q_T spectrum at N^{3}LL$'$ + N^{3}LO, both inclusively and with fiducial cuts. This is the highest order achieved to date for a differential distribution at a hadron collider. Compared to N^{3}LL, the resummation at N^{3}LL$'$ incorporates the complete $\mathcal{O}(\alpha_s^3)$ singular structure for $q_T \to 0$, i.e., all three-loop virtual and corresponding real corrections, allowing us to consistently match to N^{3}LO. We incorporate the fiducial cuts in the resummed q_T spectrum following the recent analysis in Ref. [46]. This allows us to also resum large, so-called fiducial power corrections induced by the fiducial cuts [46,47], and eventually to predict the total fiducial cross section at N^{3}LO from the integral of the resummed fiducial q_T spectrum. This constitutes the first complete application of q_T subtractions at this order. (For earlier results and discussions, see Refs. [48,49].)

The total inclusive cross section can be considered independently of the q_T spectrum. In particular, the q_T resummation effects in the inclusive spectrum formally

cancel in its integral. This cancellation is broken by the fiducial power corrections, causing leftover logarithmic contributions in the total fiducial cross section which worsen its perturbative behavior. They are resummed by integrating the resummed spectrum, restoring the perturbative convergence. Hence, the fiducial q_T spectrum is now the more fundamental quantity, while the total fiducial cross section becomes a derived quantity.

q_T resummation with fiducial power corrections.—We work in the narrow-width limit and factorize the cross section into Higgs production and decay,

$$\frac{d\sigma}{dq_T} = \int dY\, A(q_T, Y; \Theta) W(q_T, Y). \tag{2}$$

Since the Higgs is a scalar boson, Eq. (2) contains a single hadronic structure function $W(q_T, Y)$ encoding the $gg \to H$ production process. As W is a Lorentz-scalar function and inclusive over the hadronic final state, it can only depend on the Higgs momentum q^μ and the proton momenta $P^\mu_{a,b}$ via $q^2 = m_H^2$ and $2q \cdot P_{a,b} = E_{\rm cm}\sqrt{m_H^2 + \vec{q}_T^{\,2}}\, e^{\mp Y}$, where Y and $\vec{q}_T$ are the Higgs rapidity and transverse momentum. Its only nontrivial dependence is thus on Y and $q_T = |\vec{q}_T|$. The function $A(q_T, Y; \Theta)$ in Eq. (2) encodes the Higgs decay including fiducial cuts, collectively denoted by Θ. It corresponds to the fiducial acceptance point by point in q_T and Y, such that in the inclusive case without cuts $A_{\rm incl}(q_T, Y) = 1$. Hence, W is equivalent to the inclusive spectrum.

Let us expand the q_T spectrum in powers of q_T/m_H,

$$\begin{aligned}\frac{d\sigma}{dq_T} &= \frac{d\sigma^{(0)}}{dq_T} + \frac{d\sigma^{(1)}}{dq_T} + \frac{d\sigma^{(2)}}{dq_T} + \cdots \\ &\sim \frac{1}{q_T}\left[\mathcal{O}(1) + \mathcal{O}\left(\frac{q_T}{m_H}\right) + \mathcal{O}\left(\frac{q_T^2}{m_H^2}\right) + \cdots\right].\end{aligned} \tag{3}$$

The singular, leading-power term $d\sigma^{(0)}/dq_T$ scales as $1/q_T$ and dominates for $q_T \ll m_H$. It contains $\delta(q_T)$ and $[\ln^n(q_T/m_H)/q_T]_+$ distributions encoding the cancellation of real and virtual infrared singularities at $q_T = 0$. The $d\sigma^{(n\geq 1)}/dq_T$ are called power corrections.

Because of azimuthal symmetry, $W(q_T, Y)$ only receives quadratic power corrections [46,50],

$$W(q_T, Y) = W^{(0)}(q_T, Y) + W^{(2)}(q_T, Y) + \cdots, \tag{4}$$

where $W^{(0)} \sim 1/q_T$ contains the singular terms. The acceptance corrections are finite at $q_T = 0$, but the fiducial cuts generically break azimuthal symmetry such that it receives linear power corrections [46,47],

$$A(q_T, Y; \Theta) = A(0, Y; \Theta)\left[1 + \mathcal{O}\left(\frac{q_T}{m_H}\right)\right]. \tag{5}$$

The strict leading-power spectrum is thus given by

$$\frac{d\sigma^{(0)}}{dq_T} = \int dY A(0, Y; \Theta) W^{(0)}(q_T, Y). \tag{6}$$

The fiducial power corrections,

$$\frac{d\sigma^{\rm fpc}}{dq_T} = \int dY [A(q_T, Y; \Theta) - A(0, Y; \Theta)] W^{(0)}(q_T, Y), \tag{7}$$

were analyzed in Refs. [46,47]. They include all linear power corrections $d\sigma^{(1)}/dq_T$ and are absent in the inclusive spectrum. They are quite subtle, and can be further enhanced to $\mathcal{O}(q_T/p_L)$, where p_L is an effective kinematic scale set by the fiducial cuts with typically $p_L \ll m_H$. This prohibits expanding $A(q_T, Y; \Theta)$ even for $q_T \ll m_H$ once $q_T \sim p_L$. For example, for the photon $p_T^{\rm cut}$, $p_L \sim m_H - 2p_T^{\rm cut}$. For the cuts in Eq. (1), the expansion of A starts failing for $q_T \gtrsim 10$ GeV, where the inclusive power corrections from $W^{(2)}$ are at the few-percent level. It is thus critical to use the exact q_T-dependent acceptance and take

$$\frac{d\sigma^{\rm sing}}{dq_T} = \int dY\, A(q_T, Y; \Theta) W^{(0)}(q_T, Y) \tag{8}$$

as the leading "singular" contribution at small q_T, corresponding to the sum of Eqs. (6) and (7). The remaining "nonsingular" contributions,

$$\frac{d\sigma^{\rm nons}}{dq_T} = \int dY\, A(q_T, Y; \Theta)[W^{(2)}(q_T, Y) + \cdots], \tag{9}$$

are then suppressed by $\mathcal{O}(q_T^2/m_H^2)$.

In general, and for the ATLAS cuts in particular, $A(q_T, Y; \Theta)$ is a very nasty function given by a boosted phase-space integral over a conjunction of complicated θ functions encoding all cuts. Nevertheless, using a dedicated semianalytic algorithm we are able to evaluate it with sufficient numerical speed and accuracy.

As A itself does not contain large logarithms, resumming $W^{(0)}$ in Eq. (8) correctly resums also the fiducial power corrections in Eq. (7) to the same order [46]. The resummation of $W^{(0)}$ is equivalent to that of the leading-power inclusive spectrum, and follows from its factorization theorem originally derived in Refs. [51–53] or equivalent formulations [54–60]. We employ soft-collinear effective theory [61–65] with rapidity renormalization [58,66] using the exponential regulator [60], where

$$\begin{aligned}&W^{(0)}(q_T, Y) \\ &\quad = H(m_H^2, \mu) \int d^2\vec{k}_a d^2\vec{k}_b d^2\vec{k}_s \delta(q_T - |\vec{k}_a + \vec{k}_b + \vec{k}_s|) \\ &\qquad \times B_g^{\mu\nu}(x_a, \vec{k}_a, \mu, \nu) B_{g\mu\nu}(x_b, \vec{k}_b, \mu, \nu) S(\vec{k}_s, \mu, \nu).\end{aligned} \tag{10}$$

The hard function H contains the effective $gg \to H$ form factor. The beam functions $B_g^{\mu\nu}$ describe collinear radiation with total transverse momentum $\vec{k}_{a,b}$ and longitudinal momentum fractions $x_{a,b} = (m_H/E_{\rm cm})e^{\pm Y}$. The soft function S describes soft radiation with total transverse momentum $\vec{k}_s$.

All functions in Eq. (10) are renormalized objects, with μ and ν denoting their virtuality and rapidity renormalization scales. The all-order resummation follows by first evaluating each function at fixed order at its own natural boundary scale(s) $\mu_{H,B,S}$, $\nu_{B,S}$. These boundary conditions are then evolved to a common (arbitrary) point in μ and ν by solving the coupled system of renormalization group equations. The exact solution for the q_T distribution is formally equivalent [67] to the canonical solution in conjugate (b_T) space, which is the approach we follow here; see Refs. [46,67,68] for details. At N^{3}LL′ (N^{3}LL) we require the N^{3}LO (NNLO) boundary conditions for the hard [69–73] and beam and soft functions [49,74–78], the three-loop noncusp anomalous dimensions [49,74,75,79–82], and the four-loop β function [83–86] and gluon cusp anomalous dimension [87–93]. At NNLL, all ingredients enter at one order lower than at N^{3}LL.

The hard function H contains timelike logarithms $\ln[(-m_H^2 - i0)/\mu^2)]$, which are resummed by using an imaginary boundary scale $\mu_H = -im_H$. This significantly improves the perturbative convergence compared to the spacelike choice $\mu_H = m_H$ [94–98]. It is advantageous to apply this timelike resummation not just to $W^{(0)}$, which contains H naturally, but also to the full $W(q_T, Y)$, as demonstrated for the rapidity spectrum in Ref. [73], or equivalently the nonsingular corrections, as in similar contexts [81,99]. To do so, we take [73]

$$W(q_T, Y) = H(m_H^2, \mu_{\rm FO}) \left[\frac{W(q_T, Y)}{H(m_H^2, \mu_{\rm FO})}\right]_{\rm FO}, \quad (11)$$

and analogously for $d\sigma^{\rm nons}/dq_T$. The ratio in square brackets is expanded to fixed order in $\alpha_s(\mu_{\rm FO})$, while $H(m_H^2, \mu_{\rm FO})$ in front is evolved from μ_H to $\mu_{\rm FO}$ at the same order as in Eq. (10). This yields substantial improvements up to $q_T \sim 200$ GeV, which is not unexpected, as $W^{(2)}$ will contain H in parts of its factorization. (Beyond $q_T \gtrsim 200$ GeV, a dynamic hard scale $\sim q_T$ becomes more appropriate and the heavy-top limit breaks down, indicating that the hard interaction has become completely unrelated to the $H + 0$-parton process.)

The fixed-order coefficients of $d\sigma^{\rm nons}/dq_T$ for $q_T > 0$ are obtained as

$$\frac{d\sigma_{\rm FO}^{\rm nons}}{dq_T} = \frac{d\sigma_{\rm FO_1}}{dq_T} - \frac{d\sigma_{\rm FO}^{\rm sing}}{dq_T}. \quad (12)$$

At N^{n}LO ($\equiv$N^{n}LO$_0$), or $\mathcal{O}(\alpha_s^n)$ relative to the LO Born cross section, we need the full spectrum at N^{n-1}LO$_1$. At LO$_1$ and NLO$_1$, we integrate our own analytic implementation of $W(q_T, Y)$ against $A(q_T, Y; \Theta)$, allowing us to reach 10^{-4} relative precision down to $q_T = 0.1$ GeV at little computational cost. At NLO$_1$, we implement results from Ref. [100] after performing the necessary renormalization. The implementation is checked against the numerical code from Ref. [29]. At NNLO$_1$, we use existing results [41,42] from NNLOjet [30,34] (see below).

The final resummed q_T spectrum is then given by

$$\frac{d\sigma}{dq_T} = \frac{d\sigma^{\rm sing}}{dq_T} + \frac{d\sigma^{\rm nons}}{dq_T}. \quad (13)$$

While for $q_T \ll m_H$ the singular and nonsingular contributions can be considered separately, this separation becomes meaningless for $q_T \sim m_H$. To obtain a valid prediction there, the q_T resummation is switched off, only keeping the timelike resummation, by choosing common boundary scales $\mu_{S,B} = \nu_{S,B} = i\mu_H = \mu_{\rm FO}$, such that singular and nonsingular exactly recombine at fixed order into the full result. We use q_T-dependent profile scales [46,99,101] to enforce the correct q_T resummation for $q_T \ll m_H$ and smoothly turn it off toward $q_T \sim m_H$.

We identify several sources of perturbative uncertainties, namely fixed-order ($\Delta_{\rm FO}$), q_T resummation (Δ_{q_T}), timelike resummation (Δ_φ), and matching uncertainties ($\Delta_{\rm match}$), which are estimated via appropriate scale variations as detailed in Refs. [46,73]. They are considered independent sources and are consequently added in quadrature to obtain the total uncertainty. We neglect nonperturbative effects at small q_T, which are expected to be $\sim\Lambda_{\rm QCD}^2/q_T^2$ and smaller than the current perturbative uncertainties.

Our numerical results are obtained with SCETlib [102]. We use the PDF4LHC15 NNLO parton distribution functions (PDFs) [103], $\alpha_s(m_Z) = 0.118$, $\mu_{\rm FO} = m_H = 125$ GeV. We work in the top limit rescaled with the exact LO dependence on $m_t = 172.5$ GeV (rEFT). By default, we exclude the $H \to \gamma\gamma$ branching ratio ($\mathcal{B}_{\gamma\gamma}$) from our predictions, $\sigma \equiv \sigma_{\rm fid}/\mathcal{B}_{\gamma\gamma}$. Our q_T spectrum at N^{3}LL′ + N^{3}LO is presented in Fig. 1, showing excellent perturbative convergence. Below $q_T \lesssim 10$ GeV, this would not be the case without resumming the fiducial power corrections. We also compare to preliminary ATLAS measurements [26], for which we subtract the non-gluon-fusion background and divide by the photon isolation efficiency [8] and $\mathcal{B}_{\gamma\gamma}$.

Total fiducial cross section.—If (and only if) the singular distributional structure of $d\sigma^{(0)}/dq_T$ is known, the q_T spectrum can be integrated to obtain the total cross section. This is the basis of q_T subtractions [45],

$$\sigma = \sigma^{\rm sub}(q_T^{\rm off}) + \int dq_T \left[\frac{d\sigma}{dq_T} - \frac{d\sigma^{\rm sub}}{dq_T}\theta(q_T \le q_T^{\rm off})\right]. \quad (14)$$

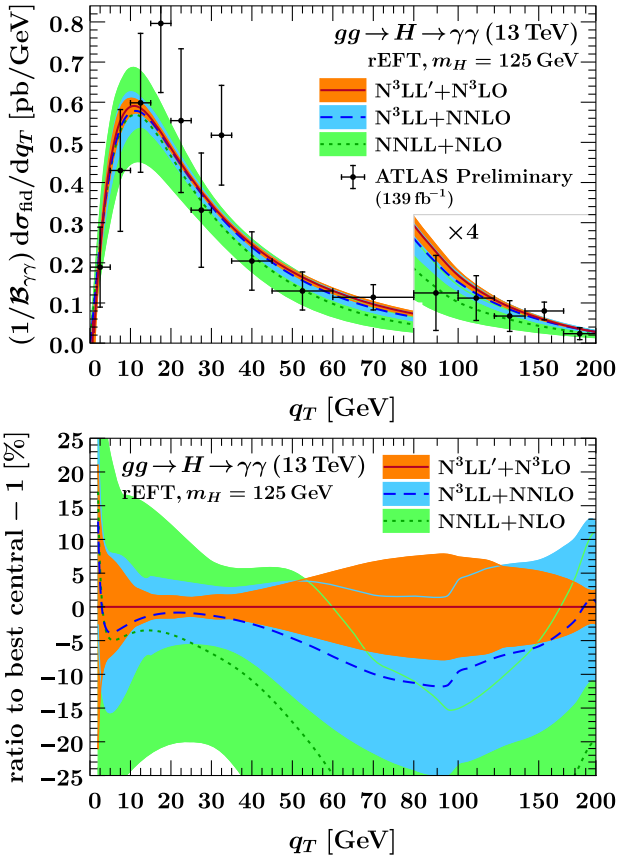

FIG. 1. The $gg \to H$ q_T spectrum up to N^{3}LL′ + N^{3}LO compared to preliminary ATLAS measurements [26].

Here, $d\sigma^{\rm sub} = d\sigma^{(0)}[1 + \mathcal{O}(q_T/m_H)]$ contains the singular terms, with $\sigma^{\rm sub}(q_T^{\rm off})$ its distributional integral over $q_T \le q_T^{\rm off}$, while the term in brackets is numerically integrable. Taking $\sigma^{\rm sub} \equiv \sigma^{\rm sing}$, we get

$$\sigma = \sigma^{\rm sing}(q_T^{\rm off}) + \int_0^{q_T^{\rm off}} dq_T \frac{d\sigma^{\rm nons}}{dq_T} + \int_{q_T^{\rm off}} dq_T \frac{d\sigma}{dq_T}, \qquad (15)$$

which is exactly the integral of Eq. (13). The subtractions here are differential in q_T, where $q_T^{\rm off} \sim 10$–100 GeV determines the range over which they act and exactly cancels between all terms.

To integrate $d\sigma^{\rm nons}/dq_T$ in Eq. (15) down to $q_T = 0$, we parametrize the fixed-order coefficients in Eq. (12) by their leading behavior,

$$q_T \frac{d\sigma_{\rm FO}^{\rm nons}}{dq_T}\bigg|_{\alpha_s^n} = \frac{q_T^2}{m_H^2} \sum_{k=0}^{2n-1} \left(a_k + b_k \frac{q_T}{m_H} + \cdots\right) \ln^k \frac{q_T^2}{m_H^2}, \qquad (16)$$

and perform a fit to this parametrization, which we then integrate analytically. We follow the fit procedure discussed in detail in Refs. [104,105] including the selection of fit parameters and range, extended to the present case. In particular, to obtain reliable, unbiased fit results, we must account for the uncertainties in the parametrization from yet higher-power corrections. This is done by including the next higher-power coefficients ($b_k, \ldots$) as nuisance parameters to the extent required by the fit range and precision. In the fiducial case, all b_k coefficients are required. The fit has been validated extensively. As a benchmark, we correctly reproduce the α_s (α_s^2) coefficients of the total inclusive cross section to better than 10^{-5} (10^{-4}) relative precision.

At N^{3}LO, we use existing NNLOjet results [41,42] to get nonsingular data for $0.74\ {\rm GeV}(4\ {\rm GeV}) \le q_T \le q_T^{\rm off}$ for inclusive log bins (for inclusive and fiducial linear bins). While these data are not yet precise enough toward small q_T to give a stable fit on their own, we exploit that in the inclusive case, the known α_s^3 coefficient of the total inclusive cross section [25,106] provides a sufficiently strong additional constraint to obtain a reliable fit. In the fiducial case, we exploit that the inclusive and fiducial a_k are related, arising from the same Y-dependent coefficient functions integrated either inclusively or against $A(0, Y; \Theta)$. At NLO and NNLO, their ratios lie between 0.4 and 0.55. At N^{3}LO, we thus perform a simultaneous fit to inclusive and fiducial data, using 12 fiducial and 8 inclusive parameters, with a loose 1σ constraint on the fiducial a_k to be 0.4–0.55 times their inclusive counterparts. (The $b_k, \ldots$ parameters are unrelated and unconstrained.) We stress that this does not amount to rescaling any part of the fiducial NNLO cross section with an inclusive N^{3}LO K factor. It merely tells the fit to only consider a_k of roughly the right expected size. This is sufficient to break degeneracies and yields a stable fit, with an acceptable ~0.1 pb uncertainty for the fiducial nonsingular integral ($\Delta_{\rm nons}$).

The often-used q_T slicing approach amounts to taking $q_T^{\rm off} \to q_T^{\rm cut} \sim 1$ GeV and simply dropping the power corrections below $q_T^{\rm cut}$. The nonsingular and fiducial power corrections are shown in Fig. 2. The latter are huge at α_s^3, and even at α_s^2 only become really negligible below

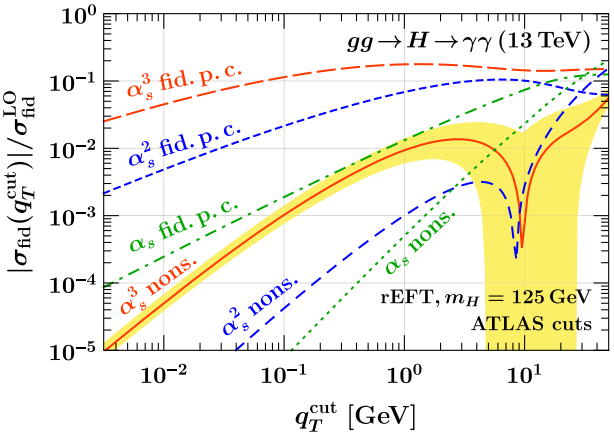

FIG. 2. Fiducial and nonsingular power corrections integrated up to $q_T \le q_T^{\rm cut}$. The yellow band shows $\Delta_{\rm nons}$ from the fit.

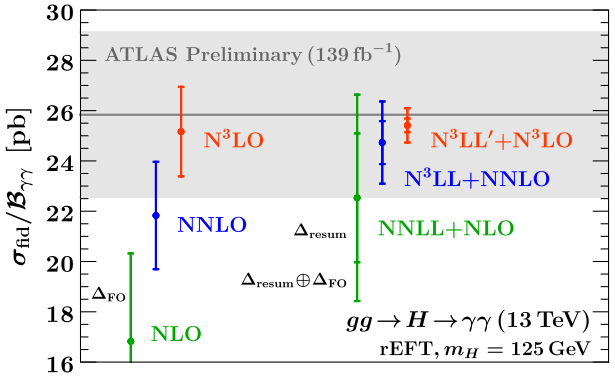

FIG. 3. Total fiducial $gg \to H \to \gamma\gamma$ cross section at fixed N^{3}LO (this work) and including resummation (also this work), where $\Delta_{\rm resum} \equiv \Delta_{q_T} \oplus \Delta_{\varphi} \oplus \Delta_{\rm match}$, compared to preliminary ATLAS measurements [26].

$q_T^{\rm cut} \lesssim 10^{-2}$ GeV. This is why it is critical for us to include them in the subtractions (and to resum them). The remaining nonsingular corrections at α_s^3 are about 10 times larger than at α_s^2, and at $q_T^{\rm cut} = 1$–5 GeV still contribute 5%–10% of the total α_s^3 coefficient. Together with the current precision of the nonsingular data, this makes the above differential subtraction procedure essential to our results.

Evaluating Eq. (15) either at fixed order or including resummation, we obtain our final results for the total fiducial cross section presented in Fig. 3. The poor convergence at fixed order is largely due to the fiducial power corrections. To see this,

$$\begin{aligned}\sigma_{\rm incl}^{\rm FO} &= 13.80[1 + 1.291 + 0.783 + 0.299]\ \text{pb},\\ \sigma_{\rm fid}^{\rm FO}/\mathcal{B}_{\gamma\gamma} &= 6.928[1 + (1.300 + 0.129_{\rm fpc})\\ &\quad + (0.784 - 0.061_{\rm fpc})\\ &\quad + (0.331 + 0.150_{\rm fpc})]\ \text{pb}. \end{aligned} \tag{17}$$

The successive terms are the contributions from each order in α_s. The numbers with "fpc" subscript are the contributions of the fiducial power corrections in Eq. (7) integrated over $q_T \le 130$ GeV. The corrections without them are almost identical to the inclusive case. The fiducial power corrections break this would-be universal acceptance effect, causing a 10% correction at NLO and NNLO and a 50% correction at N^{3}LO and showing no perturbative convergence.

Integrating $W^{(0)}$ over q_T, all q_T logarithms and resummation effects formally have to cancel. (Numerically, this strongly depends on the specific implementation of resummation and matching. We have verified explicitly that it is well satisfied in our approach.) For the fiducial power corrections, the nontrivial q_T dependence of the acceptance spoils this cancellation and induces residual logarithmic dependence on p_L/m_H in the integral. This causes the large corrections in Eq. (17), which get resummed using the resummed $\sigma^{\rm sing}$ in Eq. (15). Together with timelike resummation, this leads to the excellent convergence of the resummed results in Fig. 3, very similar to the inclusive case [73],

$$\begin{aligned}\sigma_{\rm incl} &= 24.16[1 + 0.756 + 0.207 + 0.024]\ \text{pb},\\ \sigma_{\rm fid}/\mathcal{B}_{\gamma\gamma} &= 12.89[1 + 0.749 + 0.171 + 0.053]\ \text{pb}. \end{aligned} \tag{18}$$

To conclude, our best result for the fiducial Higgs cross section at N^{3}LL′ + N^{3}LO for the cuts in Eq. (1) reads

$$\begin{aligned}\sigma_{\rm fid}/\mathcal{B}_{\gamma\gamma} &= (25.41 \pm 0.59_{\rm FO} \pm 0.21_{q_T} \pm 0.17_{\varphi}\\ &\quad \pm 0.06_{\rm match} \pm 0.20_{\rm nons})\ \text{pb}\\ &= (25.41 \pm 0.68_{\rm pert})\ \text{pb}. \end{aligned} \tag{19}$$

Multiplying by $\mathcal{B}_{\gamma\gamma} = (2.270 \pm 0.047) \times 10^{-3}$ [107–109],

$$\begin{aligned}\sigma_{\rm fid} &= 57.69(1 \pm 2.7\%_{\rm pert} \pm 2.1\%_{\mathcal{B}}\\ &\quad \pm 3.2\%_{\rm PDF+\alpha_s} \pm 2\%_{\rm EW} \pm 2\%_{t,b,c})\ \text{fb}, \end{aligned} \tag{20}$$

where we also included approximations of additional uncertainties. The PDF + α_s uncertainty is taken from the inclusive case [24,109]. For the inclusive cross section, NLO electroweak effects give a +5% correction [110], while the net effect of finite top-mass, bottom, and charm contributions is −5% (in the pole scheme we use). We can expect roughly similar acceptance corrections for both, and therefore keep the central result unchanged but include a conservative 2% uncertainty (40% of the expected correction) for each effect. Their proper treatment requires incorporating them into the resummation framework, which we leave for future work.

We are grateful to Xuan Chen for providing us with the NNLOjet results and for communication about them. We would also like to thank our ATLAS colleagues for their efforts in making the preliminary results of Ref. [26] publicly available. This work was supported in part by the Office of Nuclear Physics of the U.S. Department of Energy under Contract No. DE-SC0011090 and within the framework of the TMD Topical Collaboration, the Deutsche Forschungsgemeinschaft (DFG) under Germany's Excellence Strategy–EXC 2121 "Quantum Universe"–390833306, and the PIER Hamburg Seed Project PHM-2019-01.

Note added.—Recently, we became aware of complementary work computing fiducial rapidity spectra in Higgs production at N^{3}LO using the projection-to-Born approach [111]. The perturbative instabilities observed there are avoided here by resumming the responsible fiducial power corrections.

[1] G. Aad *et al.* (ATLAS Collaboration), Phys. Lett. B **716**, 1 (2012).
[2] S. Chatrchyan *et al.* (CMS Collaboration), Phys. Lett. B **716**, 30 (2012).
[3] G. Aad *et al.* (ATLAS Collaboration), Phys. Lett. B **726**, 88 (2013); **734**, 406(E) (2014).
[4] G. Aad *et al.* (ATLAS Collaboration), J. High Energy Phys. 09 (2014) 112.
[5] G. Aad *et al.* (ATLAS Collaboration), Phys. Lett. B **738**, 234 (2014).
[6] G. Aad *et al.* (ATLAS Collaboration), J. High Energy Phys. 08 (2016) 104.
[7] M. Aaboud *et al.* (ATLAS Collaboration), J. High Energy Phys. 10 (2017) 132.
[8] M. Aaboud *et al.* (ATLAS Collaboration), Phys. Rev. D **98**, 052005 (2018).
[9] G. Aad *et al.* (ATLAS Collaboration), Eur. Phys. J. C **80**, 942 (2020).
[10] V. Khachatryan *et al.* (CMS Collaboration), Eur. Phys. J. C **76**, 13 (2016).
[11] V. Khachatryan *et al.* (CMS Collaboration), J. High Energy Phys. 04 (2016) 005.
[12] V. Khachatryan *et al.* (CMS Collaboration), J. High Energy Phys. 03 (2017) 032.
[13] A. M. Sirunyan *et al.* (CMS Collaboration), J. High Energy Phys. 01 (2019) 183.
[14] A. M. Sirunyan *et al.* (CMS Collaboration), Phys. Lett. B **792**, 369 (2019).
[15] A. M. Sirunyan *et al.* (CMS Collaboration), J. High Energy Phys. 03 (2021) 003.
[16] M. Cepeda *et al.*, CERN Yellow Rep. Monogr. **7**, 221 (2019).
[17] S. Dawson, Nucl. Phys. **B359**, 283 (1991).
[18] A. Djouadi, M. Spira, and P. M. Zerwas, Phys. Lett. B **264**, 440 (1991).
[19] M. Spira, A. Djouadi, D. Graudenz, and P. M. Zerwas, Nucl. Phys. **B453**, 17 (1995).
[20] R. V. Harlander and W. B. Kilgore, Phys. Rev. Lett. **88**, 201801 (2002).
[21] C. Anastasiou and K. Melnikov, Nucl. Phys. **B646**, 220 (2002).
[22] V. Ravindran, J. Smith, and W. L. V. Neerven, Nucl. Phys. **B665**, 325 (2003).
[23] C. Anastasiou, C. Duhr, F. Dulat, F. Herzog, and B. Mistlberger, Phys. Rev. Lett. **114**, 212001 (2015).
[24] C. Anastasiou, C. Duhr, F. Dulat, E. Furlan, T. Gehrmann, F. Herzog, A. Lazopoulos, and B. Mistlberger, J. High Energy Phys. 05 (2016) 058.
[25] B. Mistlberger, J. High Energy Phys. 05 (2018) 028.
[26] ATLAS Collaboration, Report No. ATLAS-CONF-2019-029, 2019.
[27] D. de Florian, M. Grazzini, and Z. Kunszt, Phys. Rev. Lett. **82**, 5209 (1999).
[28] V. Ravindran, J. Smith, and W. L. V. Neerven, Nucl. Phys. **B634**, 247 (2002).
[29] C. J. Glosser and C. R. Schmidt, J. High Energy Phys. 12 (2002) 016.
[30] X. Chen, T. Gehrmann, E. W. N. Glover, and M. Jaquier, Phys. Lett. B **740**, 147 (2015).
[31] R. Boughezal, C. Focke, W. Giele, X. Liu, and F. Petriello, Phys. Lett. B **748**, 5 (2015).
[32] R. Boughezal, F. Caola, K. Melnikov, F. Petriello, and M. Schulze, Phys. Rev. Lett. **115**, 082003 (2015).
[33] F. Caola, K. Melnikov, and M. Schulze, Phys. Rev. D **92**, 074032 (2015).
[34] X. Chen, J. Cruz-Martinez, T. Gehrmann, E. W. N. Glover, and M. Jaquier, J. High Energy Phys. 10 (2016) 066.
[35] J. M. Campbell, R. K. Ellis, and S. Seth, J. High Energy Phys. 10 (2019) 136.
[36] X. Chen, T. Gehrmann, E. W. N. Glover, and A. Huss, J. High Energy Phys. 07 (2019) 052.
[37] G. Bozzi, S. Catani, D. de Florian, and M. Grazzini, Nucl. Phys. **B737**, 73 (2006).
[38] T. Becher, M. Neubert, and D. Wilhelm, J. High Energy Phys. 05 (2013) 110.
[39] D. Neill, I. Z. Rothstein, and V. Vaidya, J. High Energy Phys. 12 (2015) 097.
[40] W. Bizon, P. F. Monni, E. Re, L. Rottoli, and P. Torrielli, J. High Energy Phys. 02 (2018) 108.
[41] X. Chen, T. Gehrmann, E. W. N. Glover, A. Huss, Y. Li, D. Neill, M. Schulze, I. W. Stewart, and H. X. Zhu, Phys. Lett. B **788**, 425 (2019).
[42] W. Bizon, X. Chen, A. Gehrmann-De Ridder, T. Gehrmann, N. Glover, A. Huss, P. F. Monni, E. Re, L. Rottoli, and P. Torrielli, J. High Energy Phys. 12 (2018) 132.
[43] D. Gutierrez-Reyes, S. Leal-Gomez, I. Scimemi, and A. Vladimirov, J. High Energy Phys. 11 (2019) 121.
[44] T. Becher and T. Neumann, J. High Energy Phys. 03 (2021) 199.
[45] S. Catani and M. Grazzini, Phys. Rev. Lett. **98**, 222002 (2007).
[46] M. A. Ebert, J. K. Michel, I. W. Stewart, and F. J. Tackmann, J. High Energy Phys. 04 (2021) 102.
[47] M. A. Ebert and F. J. Tackmann, J. High Energy Phys. 03 (2020) 158.
[48] L. Cieri, X. Chen, T. Gehrmann, E. N. Glover, and A. Huss, J. High Energy Phys. 02 (2019) 096.
[49] G. Billis, M. A. Ebert, J. K. L. Michel, and F. J. Tackmann, Eur. Phys. J. Plus **136**, 214 (2021).
[50] M. A. Ebert, I. Moult, I. W. Stewart, F. J. Tackmann, G. Vita, and H. X. Zhu, J. High Energy Phys. 04 (2019) 123.
[51] J. C. Collins and D. E. Soper, Nucl. Phys. **B193**, 381 (1981); **B213**, 545(E) (1983).
[52] J. C. Collins and D. E. Soper, Nucl. Phys. **B197**, 446 (1982).
[53] J. C. Collins, D. E. Soper, and G. F. Sterman, Nucl. Phys. **B250**, 199 (1985).
[54] S. Catani, D. de Florian, and M. Grazzini, Nucl. Phys. **B596**, 299 (2001).
[55] J. Collins, *Foundations of Perturbative QCD*, Cambridge Monographs on Particle Physics, Nuclear Physics, and Cosmology (Cambridge University Press, New York, 2011).
[56] T. Becher and M. Neubert, Eur. Phys. J. C **71**, 1665 (2011).
[57] M. G. Echevarria, A. Idilbi, and I. Scimemi, J. High Energy Phys. 07 (2012) 002.
[58] J.-Y. Chiu, A. Jain, D. Neill, and I. Z. Rothstein, J. High Energy Phys. 05 (2012) 084.

[59] J. C. Collins and T. C. Rogers, Phys. Rev. D **87**, 034018 (2013).
[60] Y. Li, D. Neill, and H. X. Zhu, Nucl. Phys. **B960**, 115193 (2020).
[61] C. W. Bauer, S. Fleming, and M. E. Luke, Phys. Rev. D **63**, 014006 (2000).
[62] C. W. Bauer, S. Fleming, D. Pirjol, and I. W. Stewart, Phys. Rev. D **63**, 114020 (2001).
[63] C. W. Bauer and I. W. Stewart, Phys. Lett. B **516**, 134 (2001).
[64] C. W. Bauer, D. Pirjol, and I. W. Stewart, Phys. Rev. D **65**, 054022 (2002).
[65] C. W. Bauer, S. Fleming, D. Pirjol, I. Z. Rothstein, and I. W. Stewart, Phys. Rev. D **66**, 014017 (2002).
[66] J.-y. Chiu, A. Jain, D. Neill, and I. Z. Rothstein, Phys. Rev. Lett. **108**, 151601 (2012).
[67] M. A. Ebert and F. J. Tackmann, J. High Energy Phys. 02 (2017) 110.
[68] G. Billis, F. J. Tackmann, and J. Talbert, J. High Energy Phys. 03 (2020) 182.
[69] R. V. Harlander, Phys. Lett. B **492**, 74 (2000).
[70] P. A. Baikov, K. G. Chetyrkin, A. V. Smirnov, V. A. Smirnov, and M. Steinhauser, Phys. Rev. Lett. **102**, 212002 (2009).
[71] R. N. Lee, A. V. Smirnov, and V. A. Smirnov, J. High Energy Phys. 04 (2010) 020.
[72] T. Gehrmann, E. W. N. Glover, T. Huber, N. Ikizlerli, and C. Studerus, J. High Energy Phys. 06 (2010) 094.
[73] M. A. Ebert, J. K. L. Michel, and F. J. Tackmann, J. High Energy Phys. 05 (2017) 088.
[74] T. Lübbert, J. Oredsson, and M. Stahlhofen, J. High Energy Phys. 03 (2016) 168.
[75] Y. Li and H. X. Zhu, Phys. Rev. Lett. **118**, 022004 (2017).
[76] M.-X. Luo, T.-Z. Yang, H. X. Zhu, and Y. J. Zhu, J. High Energy Phys. 01 (2020) 040.
[77] M. A. Ebert, B. Mistlberger, and G. Vita, J. High Energy Phys. 09 (2020) 146.
[78] M.-x. Luo, T.-Z. Yang, H. X. Zhu, and Y. J. Zhu, J. High Energy Phys. 06 (2021) 115.
[79] S. Moch, J. A. M. Vermaseren, and A. Vogt, Phys. Lett. B **625**, 245 (2005).
[80] A. Idilbi, X.-d. Ji, J.-P. Ma, and F. Yuan, Phys. Rev. D **73**, 077501 (2006).
[81] C. F. Berger, C. Marcantonini, I. W. Stewart, F. J. Tackmann, and W. J. Waalewijn, J. High Energy Phys. 04 (2011) 092.
[82] A. A. Vladimirov, Phys. Rev. Lett. **118**, 062001 (2017).
[83] O. V. Tarasov, A. A. Vladimirov, and A. Yu. Zharkov, Phys. Lett. **93B**, 429 (1980).
[84] S. A. Larin and J. A. M. Vermaseren, Phys. Lett. B **303**, 334 (1993).
[85] T. V. Ritbergen, J. A. M. Vermaseren, and S. A. Larin, Phys. Lett. B **400**, 379 (1997).
[86] M. Czakon, Nucl. Phys. **B710**, 485 (2005).
[87] G. P. Korchemsky and A. V. Radyushkin, Nucl. Phys. **B283**, 342 (1987).
[88] A. Vogt, S. Moch, and J. A. M. Vermaseren, Nucl. Phys. **B691**, 129 (2004).
[89] R. N. Lee, A. V. Smirnov, V. A. Smirnov, and M. Steinhauser, J. High Energy Phys. 02 (2019) 172.
[90] J. M. Henn, T. Peraro, M. Stahlhofen, and P. Wasser, Phys. Rev. Lett. **122**, 201602 (2019).
[91] R. Brüser, A. Grozin, J. M. Henn, and M. Stahlhofen, J. High Energy Phys. 05 (2019) 186.
[92] J. M. Henn, G. P. Korchemsky, and B. Mistlberger, J. High Energy Phys. 04 (2020) 018.
[93] A. von Manteuffel, E. Panzer, and R. M. Schabinger, Phys. Rev. Lett. **124**, 162001 (2020).
[94] G. Parisi, Phys. Lett. **90B**, 295 (1980).
[95] G. F. Sterman, Nucl. Phys. **B281**, 310 (1987).
[96] L. Magnea and G. F. Sterman, Phys. Rev. D **42**, 4222 (1990).
[97] T. O. Eynck, E. Laenen, and L. Magnea, J. High Energy Phys. 06 (2003) 057.
[98] V. Ahrens, T. Becher, M. Neubert, and L. L. Yang, Phys. Rev. D **79**, 033013 (2009).
[99] I. W. Stewart, F. J. Tackmann, J. R. Walsh, and S. Zuberi, Phys. Rev. D **89**, 054001 (2014).
[100] F. Dulat, S. Lionetti, B. Mistlberger, A. Pelloni, and C. Specchia, J. High Energy Phys. 07 (2017) 017.
[101] G. Lustermans, J. K. L. Michel, F. J. Tackmann, and W. J. Waalewijn, J. High Energy Phys. 03 (2019) 124.
[102] M. A. Ebert, J. K. L. Michel, F. J. Tackmann *et al.*, Report No. DESY-17-099, 2018, http://scetlib.desy.de.
[103] J. Butterworth *et al.*, J. Phys. G **43**, 023001 (2016).
[104] I. Moult, L. Rothen, I. W. Stewart, F. J. Tackmann, and H. X. Zhu, Phys. Rev. D **95**, 074023 (2017).
[105] I. Moult, L. Rothen, I. W. Stewart, F. J. Tackmann, and H. X. Zhu, Phys. Rev. D **97**, 014013 (2018).
[106] M. Bonvini, S. Marzani, C. Muselli, and L. Rottoli, J. High Energy Phys. 08 (2016) 105.
[107] A. Djouadi, J. Kalinowski, and M. Spira, Comput. Phys. Commun. **108**, 56 (1998).
[108] A. Bredenstein, A. Denner, S. Dittmaier, and M. M. Weber, Phys. Rev. D **74**, 013004 (2006).
[109] D. de Florian *et al.* (LHC Higgs Cross Section Working Group Collaboration), arXiv:1610.07922.
[110] S. Actis, G. Passarino, C. Sturm, and S. Uccirati, Phys. Lett. B **670**, 12 (2008).
[111] X. Chen, T. Gehrmann, E. W. N. Glover, A. Huss, B. Mistlberger, and A. Pelloni, Following Letter, Phys. Rev. Lett. **127**, 072002 (2021).